

# Delayed Electron–Ion Entanglement Revealed with Zero-Area Pulses

Axel Stenquist and Jan Marcus Dahlström<sup>†</sup>

*Department of Physics, Lund University, 22100 Lund, Sweden.*

The Grobe–Eberly doublet phenomenon occurs in photoelectron distributions when the remaining ion is dressed by a field. It was recently proposed that the manifestation of the doublet can be interpreted as a signature of quantum entanglement between free photoelectrons and hybrid states of light and matter. However, the dressed state nature of the ion prevents detection of entanglement by straightforward coincidence detection. Here, we show that odd (zero-area) envelopes can modify the dynamics such that unique channel-resolved photoelectron distributions are formed. Because these distributions can be used to correlate with the internal state of the ion, our proposed scheme opens up a novel avenue for the detection of quantum entanglement, between free particles and hybrid systems.

A curious feature of zero-area pulses is that they induce transient dynamics in a two-level system, but eventually return the system to its initial state. First discovered half a century ago, in the context of propagating light pulses, through theoretical investigations [1–4] and subsequently confirmed by experimental investigations [5, 6], zero-area pulses are now a well-known concept in quantum control theory [7]. Though resonant zero-area pulses, acting like solitons, leave the system unchanged, population transfer in two-level systems can be achieved by using detuned or chirped pulses [7–9]. Over the last decades, pulse reshaping through atomic/molecular medium has moved from picosecond [10] to femtosecond timescales [11]. Recently, the generation of zero-area pulses in perfect transient absorption with attosecond pulses was reported [12]. Zero-area pulses have also been used in single-photon physics, with applications in quantum information processing [13, 14], where phase information has been retrieved with holographic, coincidence measurements [15].

Quantum entanglement and decoherence between massive particles created through the photoelectric effect have been studied using synchrotron radiation with coincidence detection [16, 17], and more recently with time-resolution provided by attosecond pulses [18–21], in atoms and small molecules. The theory of entanglement in ultrafast light-driven processes is a rapidly expanding subject [22–28]. The development of free-electron lasers (FEL) enables production of high-intensity ultrashort pulses in the extreme-ultraviolet (XUV) and X-ray regime that are utilized in a multitude of unique strong-field investigations [29–33]. Seeded FELs, such as FERMI [34], additionally provide temporal coherence, allowing for coherent control experiments [35–37]. In particular, seeded FELs allow for strong coupling at XUV wavelengths [38], which is essential for quantum operations on ultrafast timescales. Recently an investigation of quantum entanglement in the photoelectric effect, generated between photoelectrons and light-dressed atomic

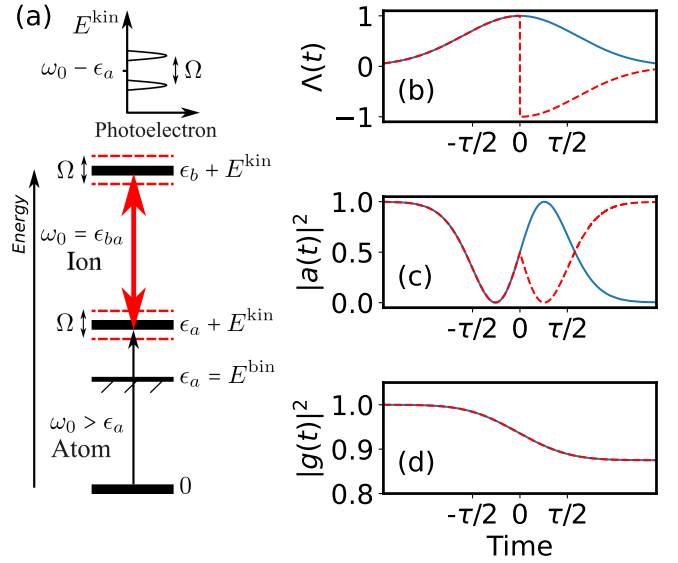


Figure 1. *Grobe–Eberly doublet and zero-area pulses.* (a) Schematic illustrating the formation of the Grobe–Eberly doublet, as due to atomic photoionization and sequential Rabi coupling in the ion. (b) Pulse envelope for a Gaussian,  $\Lambda_\tau^{\text{even}}(t)$ , (blue) and zero-Gaussian pulse,  $\Lambda_\tau^{\text{zero}}(t)$ , (red dashed). (c) Corresponding ground state population for an atom with one-photon Rabi coupling to an excited state. (d) Same as (c), but with one-photon coupling to continuum via photoionization.

ions, was conducted at FERMI [39]. In agreement with the seminal theoretical work of Grobe and Eberly [40], and more recent investigations [41–44], a doublet was observed in the photoelectron spectrum corresponding to two dressed states of the ion, as illustrated in Fig. 1(a). While the physical mechanism for this effect was attributed to quantum entanglement [39], its degree could not be measured. In fact, it would require coincidence detection of the photoelectron and ion with simultaneous quantum phase measurements — a task beyond current capabilities.

In this letter, we propose that a special class of zero-area pulses significantly reduce the complexity of detect-

<sup>†</sup> marcus.dahlstrom@matfys.lth.se

ing quantum entanglement between photoelectrons and ions in the strong-coupling regime. As we compare our results of regular and zero-area pulses, we find that: i) the generation of entanglement can be delayed and ii) the photoelectron distributions change so that electrons coupled to different ionic states “avoid each other”. The latter point opens up for coincidence detection of entanglement. Atomic units are used throughout this text,  $e = \hbar = m_e = 4\pi\epsilon_0 = 1$ , unless otherwise stated.

**Theory:** Electron dynamics are computed semi-classically, within the dipole approximation, driven by a time-dependent electric field,  $E(t) = E_0\Lambda_\tau(t)\sin(\omega_0 t)$ , where  $E_0$ ,  $\Lambda_\tau(t)$  and  $\omega_0$  are the amplitude, envelope and central frequency of the field, respectively. Additionally,  $\tau$  denotes the full width at half max of the squared envelope. In resonant interactions with two-level atoms, the interaction amplitudes:  $a(t) = \cos[\theta(t)/2]$  and  $b(t) = \sin[\theta(t)/2]$ , follow the pulse area  $\theta(t) = \int_{-\infty}^t dt' \Omega(t')$  [45], where  $\Omega(t) = z_{ba}E_0\Lambda_\tau(t) \in \mathbb{R}$  is the Rabi frequency coupling the ground state  $|a\rangle$  to the excited state  $|b\rangle$ , through the dipole matrix element,  $z_{ba}$ . Physically, the pulse area rotates the state on the Bloch sphere by the angle  $\theta(t)$  from the ground state [46]. It is useful to define the *absolute* pulse area for the total envelope:  $\theta_\tau = \int_{-\infty}^{\infty} dt|\Omega(t)|$ , as well as the *average* Rabi frequency:  $\bar{\Omega} = \int dt|\Omega(t)|^3 / \int dt|\Omega(t)|^2$ .

*Zero-area envelopes.*– The defining property of zero-area pulses is that they have a vanishing area at the end of the pulse:  $\lim_{t \rightarrow \infty} \theta(t) = 0$ . Clearly, any integrable odd function,  $\Lambda_\tau^{\text{odd}}(t) = -\Lambda_\tau^{\text{odd}}(-t)$ , satisfies this condition. In contrast, envelopes used to describe pulses in experiments are often positive even functions,  $\Lambda_\tau^{\text{even}}(t) = \Lambda_\tau^{\text{even}}(-t) \geq 0$ , such as Gaussian or flat-top pulses. Here, we consider a special class of zero-area pulses generated from even functions as  $\Lambda_\tau^{\text{zero}}(t) = \text{sign}(t)\Lambda_\tau^{\text{even}}(t)$ . In particular, we will study the Gaussian and its corresponding zero-area envelope, the “zero Gaussian”, but our conclusions generally apply to other pulse envelopes. Qualitatively similar results are also expected for smooth sign changes [7, 47]. A comparison of the  $3\pi$ -area Gaussian envelope and its corresponding zero-area envelope is presented in Fig. 1(b). The Gaussian pulse causes Rabi flopping to the excited state, while the zero-area pulse induces a time reversal of the dynamics at the centre of the pulse, bringing the population back to the ground state, as shown in Fig. 1(c). Clearly, the atomic the populations,  $|a(t)|^2$  and  $|b(t)|^2 = 1 - |a(t)|^2$ , are even functions for odd envelope pulses. The interaction amplitudes are also even functions, as is evident from their area dependence.

The photoelectric effect predicts that the kinetic energy of the photoelectron is  $E^{\text{kin}} = \omega_0 - E^{\text{bin}}$ , where  $E^{\text{bin}}$  is the binding energy of the atom. In contrast to the two-level dynamics, the photoelectric effect is Markovian, and the ionization rate is unaffected by a sudden sign

change of the envelope. In Fig. 1(d), we show that the survival probability of the atomic ground state, driven by Gaussian and zero-Gaussian pulses, are indeed identical. This is easily understood from the instantaneous photoionization rate:  $\Gamma_{ag}(t) = 2\pi|z_{ag}E_0\Lambda_\tau(t)/2|^2$ , which depends only on the square of the envelope and the coupling to the continuum,  $z_{ag}$ .

*Grobe–Eberly doublet.*– In the presence of a strongly coupled ionic resonance, Grobe and Eberly predicted a modification to the photoelectric effect: the manifestation of doublet peaks separated by the Rabi frequency [40]. Given the relative photoelectron energy,  $\epsilon = E^{\text{kin}} - (\omega_0 - E^{\text{bin}})$ , the photoelectron peaks then appear at the energies  $\epsilon_\pm = \pm\bar{\Omega}/2$ , corresponding to two final dynamically dressed ionic states.

The dynamics can be well explained using a 2-step model [44]: *-1-* The field ionizes the atom at time  $t$ , leaving the ion in the ground state and creating a photoelectron with the remaining energy. *-2-* The field induces Rabi oscillations in the ion, between the ground and excited state, while the photoelectron propagates freely. Here, we apply envelope symmetries to find the following simple expressions for the final state amplitudes:

$$\begin{aligned} c_a(\tau, \epsilon) &= \frac{\Omega_0^{ag}}{2} \int_{-\infty}^{\infty} dt a_\tau(-t)\Lambda_\tau(t)g_\tau(t)e^{i\epsilon t}, \\ c_b(\tau, \epsilon) &= \chi \frac{\Omega_0^{ag}}{2} \int_{-\infty}^{\infty} dt b_\tau^*(-t)\Lambda_\tau(t)g_\tau(t)e^{i(\epsilon - \Delta\omega)t}, \end{aligned} \quad (1)$$

where  $a_\tau(t)$ ,  $b_\tau(t)$  and  $g_\tau(t)$  are ionic and atomic interaction amplitudes, and  $\Delta\omega$  is the detuning. Envelope symmetries are accounted for by  $\chi = 1$  ( $-1$ ) for even (odd) envelopes. The density matrix for the reaction can then be constructed from  $\rho_{gg}(\tau) = g_\tau^*(\infty)g_\tau(\infty)$ ,  $\rho_{gj}(\tau; \epsilon) = g_\tau^*(\infty)c_j(\tau, \epsilon)$  and  $\rho_{jj'}(\tau; \epsilon, \epsilon') = c_j^*(\tau, \epsilon)c_{j'}(\tau, \epsilon')$ , where  $j \in \{a, b\}$ , see also supplemental material [48].

**Results:** We consider the experimentally relevant helium photoionization process, assuming the dipole matrix element  $z_{ag} = 0.502$  to be constant for the relevant photoelectron energies,  $\epsilon$ . The ionic transition between 1s and 2p has the dipole matrix element  $z_{ba} = 0.373$ , and the resonant energy  $\omega_0 = \epsilon_b - \epsilon_a = 40.2$  eV. The peak intensity of the Gaussian and zero-Gaussian envelopes is set to  $I_0 = 1.25 \cdot 10^{13}$  W/cm<sup>2</sup>, corresponding to a maximum Rabi frequency of  $\Omega_0 = z_{ba}E_0 \approx 0.2$  eV, and an average Rabi frequency of  $\bar{\Omega} \approx 0.16$  eV. Pulse durations,  $\tau$ , up to 81 fs are considered, corresponding to absolute pulse areas  $0 \leq \theta_\tau \leq 10\pi$ . First, we present the ion dynamics  $\int |c_j(\tau, \epsilon)|^2 d\epsilon$ , followed by the photoelectron spectrum  $|c_a(\tau, \epsilon)|^2 + |c_b(\tau, \epsilon)|^2$ , where  $|c_a(\tau, \epsilon)|^2$  and  $|c_b(\tau, \epsilon)|^2$  are the ion-channel resolved photoelectron probability distributions for the ground and excited state, respectively.

*Ion dynamics.*– For a Gaussian pulse, we observe oscillations in the ionic state populations as the pulse area is increased, as presented in Fig. 2(a). In contrast to the flat-top case presented in [39, 40], the oscillations are attenuated with increasing pulse area, presumably due to

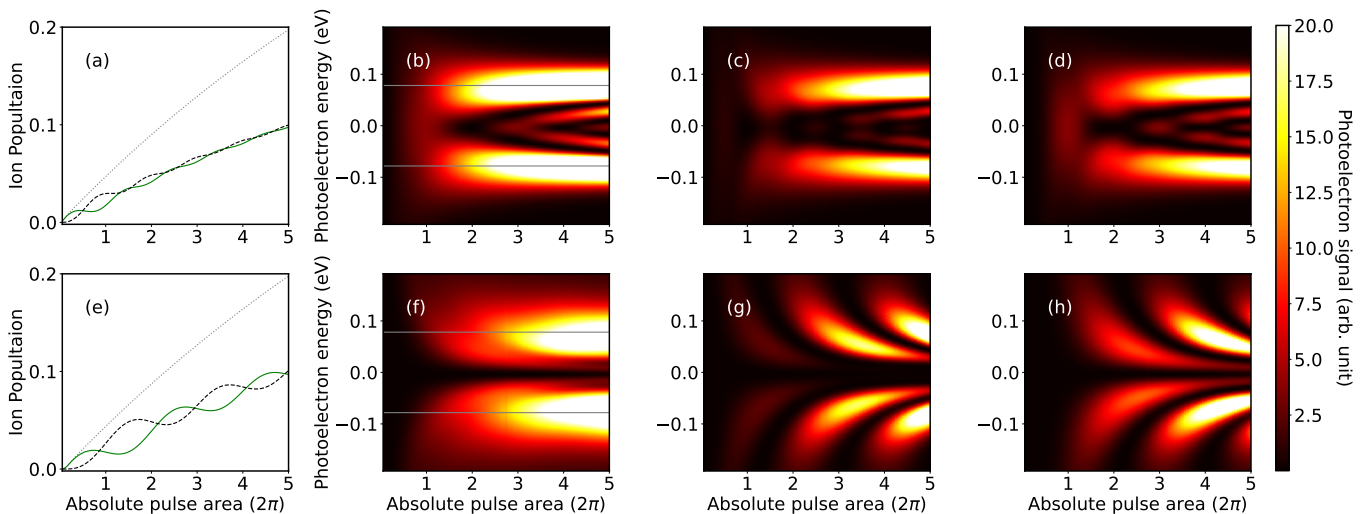


Figure 2. *Build-up of the ion dynamics and photoelectron spectra over absolute pulse area.* **Top row:** presents results for Gaussian pulses. (a) shows the ion populations of the ground state (green), the excited state (black dashed) and the full ionic population (grey dotted). The photoelectron probability distribution is presented in (b) and the ion-channel-resolved photoelectron spectra corresponding to the ground state and excited state channels are presented in (c) and (d), respectively. **Bottom row:** presents the corresponding results for the zero-Gaussian pulse. Heat maps are saturated at high photoelectron signals. Constant peak intensity and resonant frequency is used (see main text).

the range of instantaneous intensities. The number of oscillations roughly align with the pulse area in agreement with prior observations [43, 44]. In contrast, we find that for the zero-Gaussian pulse, Fig. 2(e) the ion goes through half the number of oscillations, 2.5 modulations for the absolute area of  $10\pi$ , and it shows less clear signs of attenuation.

*Photoelectron spectra.*— In Fig. 2(b), we present the pulse-area-resolved final-state photoelectron spectra for Gaussian pulses. The spectra develop from a single peak, centred on the resonant photoelectron energy,  $\epsilon = 0$ , to the dynamical Grobe–Eberly doublet,  $\pm\bar{\Omega}/2$  (grey lines). Dynamic substructures between the peaks, related to the number of completed Rabi cycles for single pulses, are observed in agreement with prior predictions for Gaussian pulses [43]. We stress that this phenomenon is closely related to two-photon resonant ionization, where it is known that the substructure is qualitatively similar for flat-top and smooth envelopes (for sufficiently small area pulses) [49, 50]. The channel-resolved photoelectron spectra are presented in (c) and (d) for the ionic ground and excited state, respectively. The doublet forms earlier in the ground state ( $\theta \approx 2\pi$ ), whereas in the excited state it forms later ( $\theta \approx 3\pi$ ) [43, 44]. The channel-resolved substructures are oscillatory, (c) and (d), but piece together to form continuous bands in the combined signal (b), similar to quantum interference effects predicted for resonant two-photon ionization [51].

In Fig. 2(f), we show that zero-Gaussian pulses yield photoelectron distributions that differ subtly from the dynamical Grobe–Eberly doublet phenomenon. Firstly,

no peak is formed at the energy  $\epsilon = 0$ , which means that the usual photoelectric pathway is “blocked”. Secondly, the photoelectron spectra for larger areas form a doublet with significantly wider peaks. Thirdly, the substructure between the doublet peaks [43] is missing in the odd envelope case. The difference between Gaussian and zero-Gaussian pulses is more striking in the channel-resolved photoelectron distributions. The two channels do not overlap, in other words: they “avoid each other”, as observed in (g) and (h) corresponding to the ground and excited state, respectively. A related splitting of the doublet peaks has been reported by Yu and Madsen for the case of two sequential pulses [44]. We attribute that effect to Ramsey-like interference, similar to the work of Wollenhaupt *et al.* on resonant photoionization [52].

*Discussion:* Here, our use of odd envelope symmetry, implies a *phase discontinuity* of the driving field [53], leading to distinct and useful behavior of the photoelectrons, as will be discussed below. While smooth even envelopes form dynamically dressed states, the dynamics from odd envelopes is different due to the associated phase discontinuity. Thus, the smooth evolution of dressed states is prevented and electron distributions with novel properties are produced.

For the zero-Gaussian pulse, the central peak does not form at  $\epsilon = 0$ . This is clear from Eq. (1) since the depletion is small,  $g_\tau(t) \approx 1$ , the envelope,  $\Lambda_\tau^{\text{zero}}(t)$ , is odd and the state amplitudes,  $j_\tau(t)$ , are even for all pulse durations. Hence, the integrand is zero, inhibiting resonant photoionization. An analytical expression for the final state amplitudes can be determined for the “zero

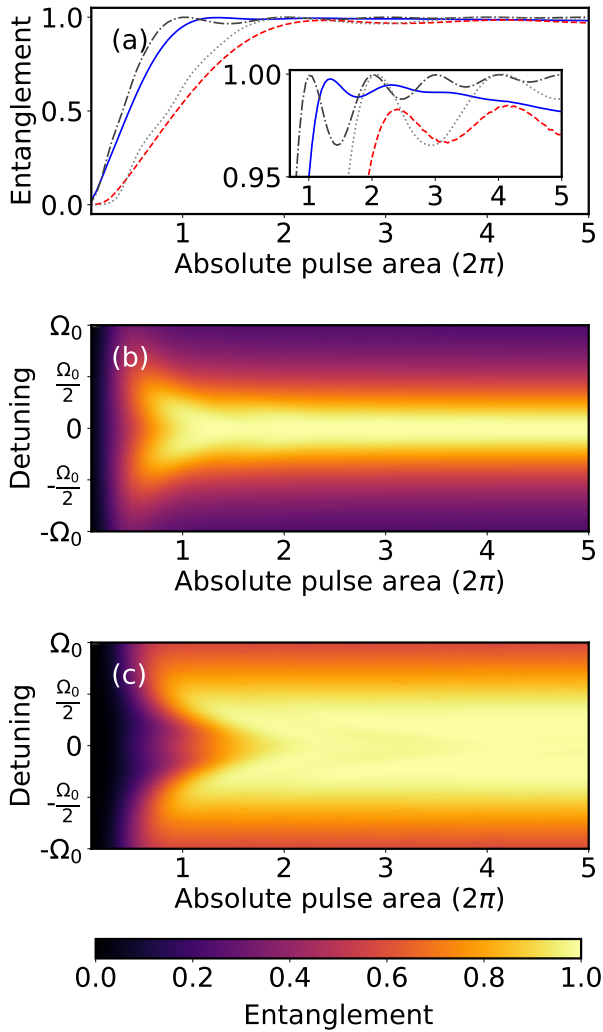


Figure 3. *Entanglement resolved over pulse area and detuning.* Absolute-pulse-area resolved entanglement (a) for a resonant Gaussian (blue) and its corresponding zero-area pulse (red dashed) as well as a flat-top (dark grey dash-dotted) and flat-top zero-area pulse (light grey dotted). Detuning- and pulse-area-resolved entanglement is presented in (b) and (c) for the Gaussian and zero-Gaussian pulses, respectively.

flat-top” envelope by neglecting depletion, as  $c_j = c_j^+ + c_j^-$ ,

$$\begin{aligned}
 c_a^\pm(\tau, \epsilon) &= \frac{i\Omega_0^{ag} \cos(\epsilon\tau/2) \pm \cos(\Omega_0\tau/4)}{2 \Omega_0/2 \mp \epsilon}, \\
 c_b^\pm(\tau, \epsilon) &= -\frac{i\Omega_0^{ag} \sin(\epsilon\tau/2) \mp \sin(\Omega_0\tau/4)}{2 \Omega_0/2 \mp \epsilon},
 \end{aligned}
 \quad (2)$$

where the origin of the doublet peaks is observed in the denominator, centred on  $\pm\Omega_0/2$ . We note that the photoelectron densities of the two channels avoid each other, due to their cosine and sine character for the ionic ground and excited state, respectively. By comparing with the analytical model for the flat-top pulse, we note that the even pulse yields oscillations at twice the frequency of the zero area pulse, as observed in Fig. 2 and Fig. 3. Further

details are found in the supplemental material [48].

*Entanglement.*— In order to analyse our results, we form the post-measurement density matrix by conditioning the full density matrix on the photoionization, by applying the projection operator  $Q = \int d\epsilon \sum_j |j, \epsilon\rangle \langle j, \epsilon|$  and renormalizing with the population of ionization,  $\text{Tr}\{\rho Q\}$ . The post-measurement density matrix is then  $\tilde{\rho} = Q\rho Q / \text{Tr}\{\rho Q\} = \sum_{jj'} \iint d\epsilon d\epsilon' \rho'_{jj'}(\tau; \epsilon, \epsilon') |j, \epsilon\rangle \langle j', \epsilon'|$ . The degree of entanglement is quantified using the Von Neumann entropy of entanglement  $S(\tau) = -\text{Tr}\{\rho^I(\tau) \log_2[\rho^I(\tau)]\}$ , where  $\rho^I(\tau) = \text{Tr}_e\{\tilde{\rho}(\tau)\}$  is the  $2 \times 2$  reduced density matrix of the ion [54]. The entanglement, resolved over pulse area, is presented in Fig. 3(a) for the Gaussian and zero-Gaussian pulse. Additionally, the flat-top envelope entanglements are given. The insert shows the entanglement between 0.95 and 1. Compared to the flat-top pulses, we see a slight delay in the build-up of entanglement for smooth pulses. In contrast, the entanglement is severely delayed in the case of zero-area pulses, where the flat top becomes fully entangled at  $\theta = 4\pi$ . The zero-area Gaussian is further slightly delayed reaching a peak entanglement of  $\sim 98\%$ .

*Detuning.*— By introducing a detuning to the pulse,  $\omega_0 = \epsilon_b - \epsilon_a + \Delta\omega$ , we can change the dynamical build-up of the entanglement. Detuning- and absolute-pulse-area-resolved entanglement is shown in Fig. 3(b) and (c) for the Gaussian and its corresponding zero-area pulse, respectively. In both cases, the entanglement decreases as the pulse is detuned and the build-up of entanglement is faster off-resonance.

*Conclusions:* In this letter, we have studied the entanglement between photoelectrons and strongly coupled ions. Our results show that odd envelopes, a special class of zero-area pulses, break the dressing mechanism of the ion and alter the photoelectron distribution. The resonant photoelectric effect is blocked and entanglement is delayed by a factor of two in terms of absolute pulse area. Despite the breakdown of dressed states, induced by zero-area pulses, the entanglement eventually reaches values close to those maximally allowed for qubit systems, but its manifestation is changed: the electrons now avoid each other when detected in coincidence with the internal states of the ion Fig. 2(g,h). Thus, our work provides key insights for future pump-probe experiments on the entanglement between electrons and coupled states of ions [23, 26, 44].

## ACKNOWLEDGEMENTS

We acknowledge discussions with Edvin Olofsson, Yijie Liao, and Saikat Nandi. JMD acknowledges support from the Olle Engkvist Foundation: 194-0734 and the Knut and Alice Wallenberg Foundation: 2019.0154.

- 
- [1] C. K. Rhodes, A. Szöke, and A. Javan, The Influence of Level Degeneracy on the Self-Induced Transparency Effect, *Phys. Rev. Lett.* **21**, 1151 (1968).
- [2] D. C. Burnham and R. Y. Chiao, Coherent Resonance Fluorescence Excited by Short Light Pulses, *Phys. Rev.* **188**, 667 (1969).
- [3] M. D. Crisp, Propagation of Small-Area Pulses of Coherent Light through a Resonant Medium, *Phys. Rev. A* **1**, 1604 (1970).
- [4] F. A. Hopf, G. L. Lamb, C. K. Rhodes, and M. O. Scully, Some Results on Coherent Radiative Phenomena with  $0\pi$  Pulses, *Phys. Rev. A* **3**, 758 (1971).
- [5] H. Grieneisen, J. Goldhar, N. Kurnit, A. Javan, and H. Schlossberg, Observation of the transparency of a resonant medium to zero-degree optical pulses, *Applied Physics Letters* **21**, 559 (1972).
- [6] S. M. Hamadani, J. Goldhar, N. A. Kurnit, and A. Javan, Coherent optical pulse reshaping in a resonant molecular absorber, *Applied Physics Letters* **25**, 160 (1974).
- [7] G. S. Vasilev and N. V. Vitanov, Complete population transfer by a zero-area pulse, *Phys. Rev. A* **73**, 023416 (2006).
- [8] J. M. S. Lehto and K.-A. Suominen, Time-dependent two-level models and zero-area pulses, *Phys. Scr.* **91**, 013005 (2016).
- [9] H.-g. Lee, Y. Song, H. Kim, H. Jo, and J. Ahn, Quantum dynamics of a two-state system induced by a chirped zero-area pulse, *Phys. Rev. A* **93**, 023423 (2016).
- [10] J. E. Rothenberg, D. Grischkowsky, and A. C. Balant, Observation of the Formation of the  $0\pi$  Pulse, *Phys. Rev. Lett.* **53**, 552 (1984).
- [11] M. Matusovsky, B. Vaynberg, and M. Rosenbluh,  $0\pi$  pulse propagation in the extreme sharp-line limit, *J. Opt. Soc. Am. B* **13**, 1994 (1996).
- [12] Y. He, Z. Liu, C. Ott, A. N. Pfeiffer, S. Sun, M. B. Gaarde, T. Pfeifer, and B. Hu, Resonant Perfect Absorption Yielded by Zero-Area Pulses, *Phys. Rev. Lett.* **129**, 273201 (2022).
- [13] S. Derouault and M. Bouchene, One-photon wavepacket interacting with a two-level atom in a waveguide: Constraint on the pulse shape, *Physics Letters A* **376**, 3491 (2012).
- [14] L. Costanzo, A. Coelho, D. Pellegrino, M. Mendes, L. Acioli, K. Casemiro, D. Felinto, A. Zavatta, and M. Bellini, Zero-Area Single-Photon Pulses, *Phys. Rev. Lett.* **116**, 023602 (2016).
- [15] M. Lipka and M. Parniak, Single-Photon Hologram of a Zero-Area Pulse, *Phys. Rev. Lett.* **127**, 163601 (2021).
- [16] D. Akoury *et al.*, The Simplest Double Slit: Interference and Entanglement in Double Photoionization of H<sub>2</sub>, *Science* **318**, 949 (2007).
- [17] M. N. Piancastelli, R. Guillemin, T. Marchenko, L. Journel, O. Travnikova, T. Marin, G. Goldsztejn, B. C. De Miranda, I. Ismail, and M. Simon, New achievements on relaxation dynamics of atoms and molecules photoexcited in the tender x-ray domain at synchrotron SOLEIL, *J. Phys. B: At. Mol. Opt. Phys.* **50**, 042001 (2017).
- [18] T. Nishi, E. Lötstedt, and K. Yamanouchi, Entanglement and coherence in photoionization of H<sub>2</sub> by an ultrashort XUV laser pulse, *Phys. Rev. A* **100**, 013421 (2019).
- [19] M. J. Vrakking, Control of Attosecond Entanglement and Coherence, *Phys. Rev. Lett.* **126**, 113203 (2021).
- [20] D. Busto *et al.*, Probing electronic decoherence with high-resolution attosecond photoelectron interferometry, *Eur. Phys. J. D* **76**, 112 (2022).
- [21] L.-M. Koll, L. Maikowski, L. Drescher, T. Witting, and M. J. Vrakking, Experimental Control of Quantum-Mechanical Entanglement in an Attosecond Pump-Probe Experiment, *Phys. Rev. Lett.* **128**, 043201 (2022).
- [22] M. V. Fedorov, M. A. Efremov, A. E. Kazakov, K. W. Chan, C. K. Law, and J. H. Eberly, Packet narrowing and quantum entanglement in photoionization and photodissociation, *Phys. Rev. A* **69**, 052117 (2004).
- [23] J.-A. You, N. Rohringer, and J. M. Dahlström, Attosecond photoionization dynamics with stimulated core-valence transitions, *Phys. Rev. A* **93**, 033413 (2016).
- [24] M. Ruberti, S. Patchkovskii, and V. Averbukh, Quantum coherence in molecular photoionization, *Phys. Chem. Chem. Phys.* **24**, 19673 (2022).
- [25] A. S. Maxwell, L. B. Madsen, and M. Lewenstein, Entanglement of orbital angular momentum in non-sequential double ionization, *Nat Commun* **13**, 4706 (2022).
- [26] K. L. Ishikawa, K. C. Prince, and K. Ueda, Control of Ion-Photoelectron Entanglement and Coherence Via Rabi Oscillations, *J. Phys. Chem. A* **127**, 10638 (2023).
- [27] M. Ruberti, V. Averbukh, and F. Mintert, Bell test of quantum entanglement in attosecond photoionization 10.48550/ARXIV.2312.05036 (2023).
- [28] P. Stammer, J. Rivera-Dean, A. Maxwell, T. Lamprou, A. Ordóñez, M. F. Ciappina, P. Tzallas, and M. Lewenstein, Quantum Electrodynamics of Intense Laser-Matter Interactions: A Tool for Quantum State Engineering, *PRX Quantum* **4**, 010201 (2023).
- [29] L. Young *et al.*, Femtosecond electronic response of atoms to ultra-intense X-rays, *Nature* **466**, 56 (2010).
- [30] E. Lindroth, F. Calegari, L. Young, M. Harmand, N. Dudovich, N. Berrah, and O. Smirnova, Challenges and opportunities in attosecond and XFEL science, *Nat Rev Phys* **1**, 107 (2019).
- [31] L. Young *et al.*, Roadmap of ultrafast x-ray atomic and molecular physics, *J. Phys. B: At. Mol. Opt. Phys.* **51**, 032003 (2018).
- [32] A. Rudenko *et al.*, Femtosecond response of polyatomic molecules to ultra-intense hard X-rays, *Nature* **546**, 129 (2017).
- [33] E. P. Kanter *et al.*, Unveiling and Driving Hidden Resonances with High-Fluence, High-Intensity X-Ray Pulses, *Phys. Rev. Lett.* **107**, 233001 (2011).
- [34] E. Allaria *et al.*, Highly coherent and stable pulses from the FERMI seeded free-electron laser in the extreme ultraviolet, *Nature Photon* **6**, 699 (2012).
- [35] M. Fushitani, C.-N. Liu, A. Matsuda, T. Endo, Y. Toida, M. Nagasono, T. Togashi, M. Yabashi, T. Ishikawa, Y. Hikosaka, T. Morishita, and A. Hishikawa, Femtosecond two-photon Rabi oscillations in excited He driven by ultrashort intense laser fields, *Nature Photon* **10**, 102 (2016).
- [36] K. C. Prince *et al.*, Coherent control with a short-wavelength free-electron laser, *Nature Photon* **10**, 176 (2016).
- [37] P. K. Maroju *et al.*, Attosecond coherent control of electronic wave packets in two-colour photoionization using a novel timing tool for seeded free-electron laser, *Nat. Photon.* **17**, 200 (2023).

- [38] S. Nandi *et al.*, Observation of Rabi dynamics with a short-wavelength free-electron laser, *Nature* **608**, 488 (2022).
- [39] S. Nandi *et al.*, Generation of entanglement using a short-wavelength seeded free-electron laser, *Sci. Adv.* **10**, eado0668 (2024).
- [40] R. Grobe and J. H. Eberly, Observation of coherence transfer by electron-electron correlation, *Phys. Rev. A* **48**, 623 (1993).
- [41] B. Walker, M. Kaluža, B. Sheehy, P. Agostini, and L. F. DiMauro, Observation of Continuum-Continuum Autler-Townes Splitting, *Phys. Rev. Lett.* **75**, 633 (1995).
- [42] L. G. Hanson, J. Zhang, and P. Lambropoulos, Manifestations of atomic and core resonances in photoelectron energy spectra, *Phys. Rev. A* **55**, 2232 (1997).
- [43] S. B. Zhang and N. Rohringer, Photoemission spectroscopy with high-intensity short-wavelength lasers, *Phys. Rev. A* **89**, 013407 (2014).
- [44] C. Yu and L. B. Madsen, Core-resonant ionization of helium by intense XUV pulses: Analytical and numerical studies on channel-resolved spectral features, *Phys. Rev. A* **98**, 033404 (2018).
- [45] S. L. McCall and E. L. Hahn, Self-Induced Transparency by Pulsed Coherent Light, *Phys. Rev. Lett.* **18**, 908 (1967).
- [46] R. P. Feynman, F. L. Vernon, and R. W. Hellwarth, Geometrical Representation of the Schrödinger Equation for Solving Maser Problems, *Journal of Applied Physics* **28**, 49 (1957).
- [47] Y.-M. He, H. Wang, C. Wang, M.-C. Chen, X. Ding, J. Qin, Z.-C. Duan, S. Chen, J.-P. Li, R.-Z. Liu, C. Schneider, M. Atatüre, S. Höfling, C.-Y. Lu, and J.-W. Pan, Coherently driving a single quantum two-level system with dichromatic laser pulses, *Nat. Phys.* **15**, 941 (2019).
- [48] See Supplemental Material [url] for details on the theoretical methods and the physical phenomena investigated,.
- [49] R. Rogus and M. Lewenstein, Resonant ionisation by smooth laser pulses, *J. Phys. B: Atom. Mol. Phys.* **19**, 3051 (1986).
- [50] N. S. Simonović, D. B. Popović, and A. Bunjac, Manifestations of Rabi Dynamics in the Photoelectron Energy Spectra at Resonant Two-Photon Ionization of Atom by Intense Short Laser Pulses, *Atoms* **11**, 20 (2023).
- [51] E. Olofsson and J. M. Dahlström, Photoelectron signature of dressed-atom stabilization in an intense XUV field, *Phys. Rev. Research* **5**, 043017 (2023).
- [52] M. Wollenhaupt, A. Assion, O. Bazhan, C. Horn, D. Liese, C. Sarpe-Tudoran, M. Winter, and T. Baumert, Control of interferences in an Autler-Townes doublet: Symmetry of control parameters, *Phys. Rev. A* **68**, 015401 (2003).
- [53] M. Wollenhaupt, A. Präkelt, C. Sarpe-Tudoran, D. Liese, and T. Baumert, Quantum control by selective population of dressed states using intense chirped femtosecond laser pulses, *Appl. Phys. B* **82**, 183 (2006).
- [54] S. Haroche and J.-M. Raimond, *Exploring the quantum: atoms, cavities, and photons*, first published in paperback ed., Oxford graduate texts (Oxford University Press, Oxford, 2013).